Comparison of Superconducting Generators and Permanent Magnet Generators for 10-MW Direct-Drive Wind Turbines

Liu, Dong; Polinder, Henk; Abrahamsen, Asger Bech; Wang, Xuezhou; Ferreira, Bram

Publication date
2017

Published in
19th International Conference on Electrical Machines and Systems, ICEMS 2016

Citation (APA)
Liu, D., Polinder, H., Abrahamsen, A. B., Wang, X., & Ferreira, B. (2017). Comparison of Superconducting Generators and Permanent Magnet Generators for 10-MW Direct-Drive Wind Turbines. In *19th International Conference on Electrical Machines and Systems, ICEMS 2016* (pp. 1-6). IEEE.

Comparison of Superconducting Generators and Permanent Magnet Generators for 10-MW Direct-Drive Wind Turbines

Dong Liu*, Henk Polinder*, Asger B. Abrahamsen**, Xuezhou Wang* and Jan A. Ferreira*
* Department of Electrical Sustainable Energy, Delft University of Technology, Netherlands.
** DTU Wind Energy, Technical University of Denmark, Denmark.

***Abstract*-- Large offshore direct-drive wind turbines of 10-MW power levels are being extensively proposed and studied because of a reduced cost of energy. Conventional permanent magnet generators currently dominating the direct-drive wind turbine market are still under consideration for such large wind turbines. In the meantime, superconducting generators (SCSGs) have been of particular interest to become a significant competitor because of their compactness and light weight. This paper compares the performance indicators of these two direct-drive generator types in the same 10-MW wind turbine under the same design and optimization method. Such comparisons will be interesting and insightful for commercialization of superconducting generators and for development of future wind energy industry, although SCSGs are still far from a high technology readiness level. The results show that the SCSGs may not be too expensive regarding capital cost of energy. If other major costs and reliability factors related to superconductivity are taken into consideration, however, the SCSGs may not be competitive yet at the moment.**

***Index Terms*—Cost of energy, permanent magnet, superconducting generator, wind turbine.**

I. Introduction

Direct-drive wind turbines of 10-MW power levels are being extensively proposed and studied to reduce the cost of energy of offshore wind farms. Conventional permanent magnetic synchronous generators (PMSG), which are dominating the current direct-drive wind turbine markets, are still under consideration for such large wind turbines. In the meantime, superconducting synchronous generators (SCSG) have been of particular interest to become a significant competitor, because of their compactness and light weight [1, 2].

At this moment, however, the technology readiness level of superconducting wind generators is so low that commercialization of SCSGs has not been realized yet. Comparing SCSGs to technically mature PMSGs may not be fully fair, but it will be very interesting to compare their important performance indicators (PIs) based on the same design and optimization method. Such comparisons are expected to provide feasibility insights for commercialization of SCSGs and to draw attention from the wind energy industry.

This work is part of the INNWIND.EU project supported by the FP7 framework of EU, under grant agreement No. 308974.

Fig. 1. Proposed 10-MW reference wind turbine. [3]

The objective of this paper is to compare SCSGs and a PMSGs for 10-MW direct-drive wind turbines. Firstly we design an SCSG and a PMSG through the same design and optimization method for the minimum cost of energy (CoE). Both the designed generators operate with the same wind turbine, wind condition and phasor diagram, and the optimization combines finite element (FE) and analytical models. Then the paper compares the PIs of the two generator designs with each other and another PMSG design available in the literature [4]. This PMSG design is compared as a reference since it employed a different design method established before. The PIs for comparison are: generator sizes, capital CoE of the wind turbine, annual energy production (AEP), and generator active material costs and masses.

II. Generator Design

A. General parameters

An SCSG and a PMSG are designed under the conditions for a 10-MW reference direct-drive wind turbine (Fig. 1). The rated rotational speed is 9.6-rpm. The generator is directly connected to a back-to-back power electronic converter through a no-load line voltage of 3300 V (electromotive force of 1905 V). The generator parameters are listed in Table I.

The diameter of the generator is not easy to decide. It is always a question whether to enlarge the diameter to around 10-m or to limit the diameter to a compact level (e.g. 6 m) for both the generator types. The diameter of 10 m or even larger has been extensively proposed for 10-MW direct-drive PMSGs [4-6] while a smaller

diameter is considered to take more advantage of superconductivity for an SCSG.

This paper considers both 6 m and 10 m as the air gap diameter of the SCSG and the PMSG. The diameter of 6 m may be too small for PMSGs, but it could indicate whether superconductivity is beneficial for reducing generator sizes and weights. Accordingly, the air gap length is set to 0.1% of the diameter, which is 6 mm for 6 m diameter and 10 mm for 10 m diameter.

TABLE I
GENERAL CHARACTERISTICS OF THE GENERATOR

Parameter	Value
Nominal torque	10.54 MNm
Electromotive force	1905 V
Air gap diameter	6 m or 10 m
Armature winding type	Distributed
Rated RMS armature current density	3 A/mm^2
Armature slot fill factor	0.6

The electrical loading of the armature winding is constrained below 75 kA/m to enable the use of forced air cooling for the stator. Direct cooling is costly and water cooling is complex for the wind turbine nacelle.

Two PMSG designs were proposed in [4] (for pitch control and active speed stall control, respectively) for a slightly different 10-MW wind turbine. The air gap diameter was 10 m. We select the pitch control design for the comparison in this paper since most new wind turbines adopt pitch control nowadays. The generator design can be found in [4] in great detail.

B. Operation of wind turbine and generator

The wind speed condition follows a Weibull distribution (shape factor k=2, scaling factor A=10.39). The wind turbine operate following the rotational speed and power as a function of wind speed as shown in Fig. 2. The generator is operated under the phasor diagram given in Fig. 3, which is fully controlled by the power electronic converter. The control strategy is zero d-axis control with which the d-axis current of the generator remains zero and the torque is proportional to the q-axis current. The major advantage of this control strategy is relatively low copper losses in the armature winding.

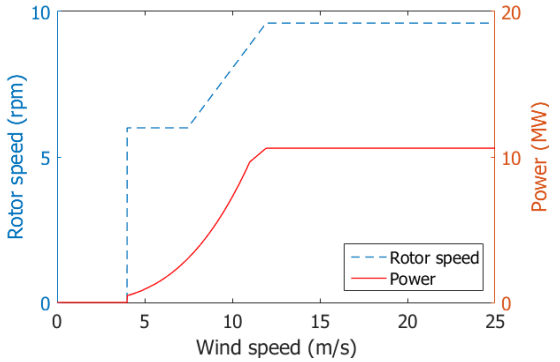

Fig. 2. Wind turbine operation (rotor speed and aerodynamic power).

C. SCSG

The SCSG design adopts the partially superconducting concept due to excessive AC losses in a superconducting armature winding. The SCSG has a DC superconducting field winding with MgB_2 superconductors and a conventional AC armature winding with copper conductors. MgB_2 superconductors are cheaper than high temperature superconductors (HTS's) but require less rigorous temperatures than low temperature superconductors (LTS's). For simplifying the cryogenic cooling effort, the operating temperature for the MgB_2 field winding is set to 20 K.

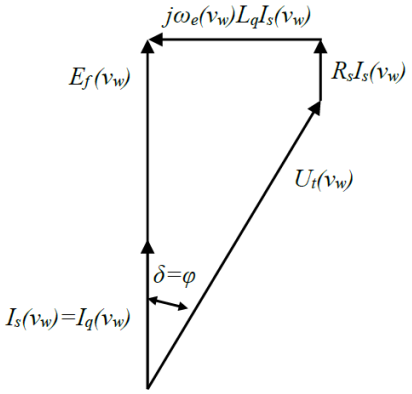

Fig. 3. Generator phasor diagram for zero d-axis current control.

The SCSG design employs a fully iron-cored topology with salient iron poles (Fig. 4). This concept is enabled with modular cryostats proposed by [7] and can effectively increase the air gap magnetic field. The size of the field coil and the cryostat together determine the size of the pole core. We assume that the cryostat takes up 40 mm space between the field coil and its warm surrounding. Due to heavy saturation, a pole shoe is not necessary from electromagnetics point of view.

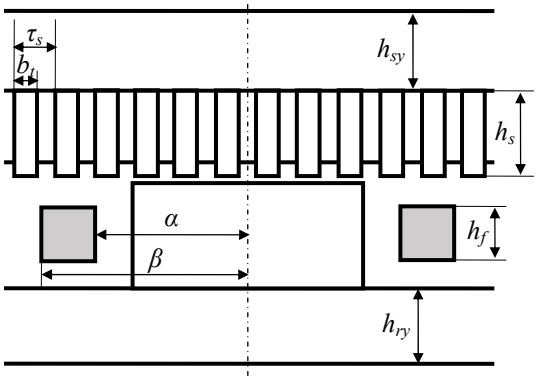

Fig. 4. Sketch of one pole of the SCSG with the notations of the optimization variables. The gray blocks are the superconducting field coil accommodated in a modular cryostat. The space left around the field coil is fixed and occupied by the modular cryostat.

The superconducting field winding of an SCSG is prone to AC losses when the field current is regulated as the way that a conventional electrically excited synchronous generator does. Thus, the field current must be changed sufficiently slowly and is changed only for regulations in hours or days. In this paper, we assume a constant field current of rated value throughout the full range of wind speed to neglect the field current regulation process at partial load.

The rated field current is determined by crossing the load line of the maximum magnetic flux density in a field coil and the critical B-J characteristic of the MgB_2 wire at 20 K with a safety margin of 25%, as illustrated in Fig. 5.

The number of slots per pole per phase in the stator is set to q=4 to reduce the slotting effect on the AC losses in the superconductors and the field winding assembly.

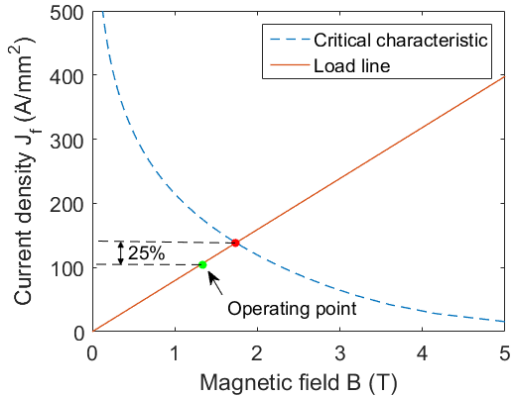

Fig. 5. Determination of the operating current density for the superconducting field winding by crossing the critical B-J characteristic of the MgB_2 wire at 20 K and the load line of the field winding, taking a safety margin of 25% into account.

D. PMSG

The PMSG has surface-mounted permanent magnets on the rotor. The remanent magnetic flux density of the magnets is B_r=1.2 T. The number of slots per pole per phase in the stator is set to q=2 to allow for smaller pole pitches and achieve low losses in the magnets. One pole of the PMSG is sketched in Fig. 6.

The PMSG optimized in this paper is referred to as PMSG-O and the referenced PMSG designed in [4] is referred to as PMSG-R. The PMSG-R design from [3] has an armature slot filling factor of 0.65 instead of 0.60. To constrain the electrical loading no higher than 75 kA/m and the armature tooth no narrower than 2 cm (b_t≥20 mm), we adjust the original design a bit: the slot height increases from 80 mm to 106 mm, and the ratio of armature tooth width to slot pitch increases from 0.50 to 0.61. The armature filling factor is changed to 0.60. Other design parameters remain the same. This adjustment makes sure that all the generator designs to be compared comply with the same conditions and constraints.

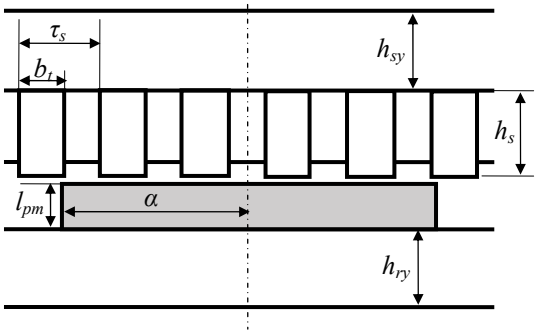

Fig. 6. Sketch of one pole of a PMSG with the notations of the optimization variables. The gray block is a permanent magnet.

III. Generator Optimization

A. Objective function

Either generator type is optimized for its minimum capital CoE of the 10-MW wind turbine. Only the capital costs are considered since the installation, operation and maintenance costs are unknown yet for 10-MW offshore wind turbines. In addition, to design a dynamically stable 10-MW wind turbine, a small tower head mass may not be desired due to natural frequency issues. Thus. The generator mass is thus not part of the optimization objective.

The component costs of the wind turbine excluding the generator, as summarized in Table II, are assumed constant. The generator cost needs to be minimized through the optimization and consists of active material cost C_{act} and structural material cost C_{str}. The cost of energy is thus defined by

$$CoE(\mathrm{X}) = \frac{C_{act}(\mathrm{X}) + C_{str}(\mathrm{X}) + C_{cryo} + C_{PE} + C_{other}}{AEP \cdot T_{life}} \qquad (1)$$

where C_{cryo} is the cost of the cryogenic system which only applies to the SCSG, C_{PE} is the cost of the power electronic converter, AEP is the annual energy production and T_{life}=25 years is the design lifetime of the wind turbine. X is the set of optimization variables.

Due to that the cryogenic system design is unknown yet for the SCSG and modeling its cost C_{cryo} is beyond the scope of this paper, we assume a fixed C_{cryo} for the SCSG which is roughly estimated from a 12-MW LTS generator proposal in [8]. This cost may be an overestimation since usually LTS generators require a more rigorous cryogenic system than the generators using MgB_2. This cost may also be an underestimation since modular cryostats may be quite costly.

TABLE II
Cost Estimation for the 10 MW Reference Wind Turbine

Component	Estimated cost		
Generator type	SCSG	PMSG-O	PMSG-R
Wind turbine (exl. generator)	7500 k€ [3]		
Balance of plant	17000 k€ [3]		
Power electronic converter C_{PE}	800 k€		
Cryogenic system C_{cryo}	1160 k€	n/a	n/a
Generator structural material C_{str}	500 k€ (6 m); 700 k€ (10 m)	To be optimized	890 k€*
Generator active material C_{act}	To be optimized	To be optimized	670 k€**

* C_{str}=708 k€ in [3], but in this paper is it calculated with Eq. (2).
** The unit cost of magnets is adapted from 25 €/kg to 50 €/kg.

Due to that the mechanical design is unknown yet for the SCSG and modeling the structural material cost C_{str} for SCSGs is beyond the scope of this paper, we assume a fixed C_{str} for the SCSG which is roughly estimated from 10-MW PMSG proposals in [5] and [9]. This cost may be an underestimation since an SCSG may have larger magnetic forces between the rotor and stator than PMSGs. This cost may also be an overestimation since the SCSG have a smaller diameter (except the 10-m SCSG) which could simplify the supporting structures.

For the PMSGs, we use a scaling function used in [10] and [5] estimate the structural material mass:

$$C_{str}(\mathrm{X}) = 0.5 c_{str,ref}\left[\left(\frac{D}{D_{ref}}\right)^3 + \left(\frac{L(\mathrm{X})}{L_{ref}}\right)^3\right] \qquad (2)$$

where D and L are the generator's air gap diameter and active axial length. The cost C_{str} is scaled from a

reference machine with a structural material cost of $c_{str,ref}$=150 k€, a diameter of D_{ref}=5 m and an active axial length of L_{ref}=1.19 m. The purpose of adding C_{str} to the optimization is not to exactly calculate the structural material cost but to limit the aspect ratio of the generator as a penalty factor.

In this paper, we assume the following unit costs for the active materials for calculating C_{act}:

- MgB_2 superconductor: 4 €/m,
- Copper conductor: 15 €/kg,
- Iron core: 3 €/kg, and
- Permanent magnet (NdFeB): 50 €/kg.

The AEP is calculated following the wind turbine rotation and power input as depicted in Fig. 2.

B. Power losses

The AEP is determined by the power losses in the generator system. Assuming that mechanical losses, e.g. bearing and windage losses, are neglected, all the aerodynamic power reaches the generator $P_{in}=P_{as}$. In the three generator types, the common power loss comes from

- Joule copper losses in the armature winding $P_{Cus,joul}$,
- Eddy current losses in the armature winding copper $P_{Cus,eddy}$, and
- Iron core losses P_{Fes} in the stator, assuming negligible iron core losses in the rotor.
- As a part of a generator system, a power electronic converter also produces a loss P_{conv}, which reduces the efficiency of a generator system.

In the SCSG, both DC and AC losses in the superconducting winding are negligibly small, according to the study in [11]. Thus, these losses are not considered. In addition, the refrigeration for cooling the cryogenic environment for superconducting wires demands a power at an ambient temperature, which can also be considered as a power loss P_{cryo}.

In the PMSG, the losses in the rotor part are negligible. Due to light saturation in the armature teeth, the eddy current losses in the armature winding copper $P_{Cus,eddy}$ can be neglected.

The total loss of the generator system is calculated by

$$P_{loss,SCSG} = P_{Cus,joul} + P_{Cus,eddy} + P_{Fes} + P_{conv} + P_{cryo} \quad (3)$$

for the SCSG.

$$P_{loss,PMSG} = P_{Cus,joul} + P_{Fes} + P_{conv} \quad (4)$$

for the PMSG.

The joule copper losses $P_{Cu,joul}$ as a function of wind speed is given by

$$P_{Cus,joul} = 3I_s^2 R_s \quad (5)$$

where I_s is the phase current and the field current, respectively, R_s is the electrical phase resistance and field resistance, respectively, at the operating temperature of about 120 ˚C.

The copper loss $P_{Cus,eddy}$ due to induced eddy currents can be effectively reduced by stranding the copper conductors. Due to heavy saturation in an SCSG, special attention must be paid to the stranding of copper conductors. There are models which can estimate the eddy current loss in copper strands if the dimension of a strand is known. Here we use the model given in [12]:

$$P_{Cu,eddy} = \frac{1}{24\rho_{Cu}} \omega_e^2 (a^2 B_r^2 + b^2 B_t^2) V_{Cus} \quad (6)$$

where ω_e is the angular electrical, B_r and B_t are the radial and tangential components of the flux density (amplitude) in the copper conductor in an armature slot, V_{Cus} is the copper volume only in the stack length, and a and b are the height and width of a copper strand. In this paper, we use finely stranded copper conductors with a=b=5 mm.

Iron core losses come from hysteresis losses and eddy current losses both of which are functions of flux density and frequency. The total iron loss per unit mass can be modeled by

$$P_{Fe} = 2[(\frac{B_r}{1.5})^2 + (\frac{B_t}{1.5})^2][k_h(\frac{f}{50}) + k_e(\frac{f}{50})^2] \quad (7)$$

where k_h=2 W/kg and k_e=0.5 W/kg are respectively the hysteresis loss and the eddy current loss per unit iron mass with the field of 1.5 T and the frequency of 50 Hz. B_r and B_t are respectively the radial and tangential components of the flux density (amplitude) in the iron core, and $f=2\pi\omega_e$ is the electrical frequency. The empirical factor of 2 in the front of (7) mainly takes into account deterioration of the laminates due to fabrication.

The cryogenic cooling power for the SCSG is estimated as 0.5% of the rated power of the superconducting generator. This estimation is based on the technical report by GE for a low-temperature superconducting generator design [13], which calculated the cryogenic cooling power at different wind speeds. This report shows that the cryogenic cooling power is constant with wind speed and it value is 22.5 kW. Since the thermal loads in the cryostat remains almost the same with wind speed changes, we assume a constant cryogenic cooling power of P_{cryo}=50 kW at all wind speeds. This power value is more than doubled 22.5 kW to consider tolerances.

The loss of the power electronic converter is modeled based on the current flowing in the power electronic switches [14] and given by

$$P_{conv} = \frac{P_{convm}}{31}(1 + 10\frac{I_s}{I_{sm}} + 5\frac{I_s^2}{I_{sm}^2} + 10\frac{I_g}{I_{gm}} + 5\frac{I_g^2}{I_{gm}^2}) \quad (8)$$

where P_{convm} is the loss in the converter at rated power (assuming 2% of the rated power of the converter), I_s is the generator side converter current, I_{sm} is the maximum generator side converter current, I_g is the grid side converter current, and I_{gm} is the maximum grid side converter current.

C. Optimization variables and method

The optimization variables for the SCSG and PMSG are listed in Table III. The notations of the variables are illustrated in Figs. 4 and 6.

The optimization is carried out in a program combining FE and analytical models. The FE models are used to calculate the magnetic field and electromagnetic

torque. The analytical models are used to calculate voltages, currents and losses. Using FE methods is to more accurately model the saturation in the iron core, especially for the SCSG which is likely to heavily saturate. This saturation is hard to model analytically since it covers linear low-field (e.g. $\mu_r \approx 4000$), nonlinear medium field (e.g. μ_r changing from 4000 to 1) and linear high field regions ($\mu_r \approx 1$) of the iron core. Although PMSGs can be modeled with analytical equations considering slotting and saturation, this paper uses FE for both the generator types to provide the same modeling and optimization conditions.

The optimization applies a genetic algorithm NSGA-II, so all the optimization variables can be integer and their step sizes of evolution can be manipulated. The number of individuals per generation is set to 50. Each individual is a set of the optimization variables' values. The optimization process will proceed until all the individuals converge to the same minimum objective. Different initial individuals are used to check if the optimum is global.

TABLE III
OPTMIZATION VARIABLES AND THEIR OPTIMAL VALUES

		SCSG		PMSG-O	
	Air gap diameter D_s (m)	6	10	6	10
	Generator active length l_s (m)	2.51	1.15	2.87	1.53
x_1	Pole pair number p	22	38	40	94
x_2	Inner pole span angle α (electrical degree)	68	66	76	72
x_3	Outer pole span angle β (electrical degree)	72	72	n/a	n/a
x_4	Field coil height h_f or magnet length l_m (mm)	14	10	46	28
x_5	Armature slot height h_s (mm)	108	114	104	118
x_6	Ratio of armature tooth width to slot pitch b_t/τ_s	0.62	0.65	0.60	0.65
x_7	Armature yoke height h_{sy} (mm)	110	114	72	60
x_8	Field yoke height h_{ry} (mm)	112	108	74	38

IV. COMPARISON RESULTS

The optimal values of the optimization variables are listed in Table III. The benefit of using superconductors to reduce the generator size can be observed but is small for the same diameter. The SCSGs need thicker stator and rotor yokes to reduce the capital CoE while the PMSGs show a feature of smaller outer diameters. With the optimized geometry, the SCSGs use a resulting field current density in the MgB_2 wire of 194 A/mm^2 for both D_s=6 m and 10 m.

The optimal SCSG and PMSG-O have had their respective minimum capital CoEs and are compared in Fig. 7 with each other and with the PMSG-R design. The capital CoE of the PMSG-R design is calculated with the identical assumptions and conditions for the SCSG and PMSG-O designs. The 10-m PMSGs are much cheaper than the SCSGs and the 6-m PMSG-O. The SCSGs are about 5% more expensive than the 10-m PMSGs even if the air gap diameter is increased to 10 m.

The AEP, used to indicate the capacity factor (CF) of a wind turbine, is extracted from the capital CoE and compared in Fig. 8. All the generators have CFs over 0.5 but only the 10-m generators have CFs over 0.51.

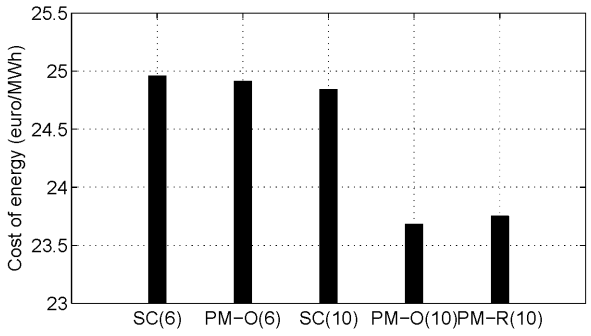

Fig. 7. Capital CoE for SCSGs, PMSG-Os and PMSG-R.

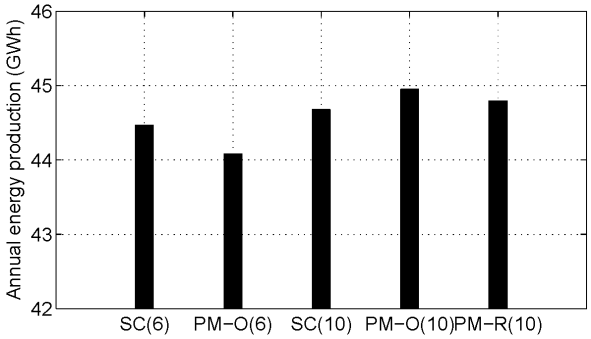

Fig. 8. AEP for SCSGs, PMSG-Os and PMSG-R. The resulting capacity factors are 0.508, 0.503, 0.510, 0.513 and 0.511, respectively.

The total generator material cost is compared in Fig. 9 which breaks down the total cost into the active material, structural material and cryostat costs. The 6-m PMSG-O seems much less competitive than its 10-m compatriots. The benefit of increasing the diameter for the SCSG is negligible because the high cryostat cost remains the same and because the summation of the active and structural material costs hardly changes. The two 10-m PMSGs show almost the same low generator costs, which are roughly 33% cheaper than the SCSGs. Compared to the scaling function in (2), the estimated structural costs in Table II for the SCSGs are underestimated.

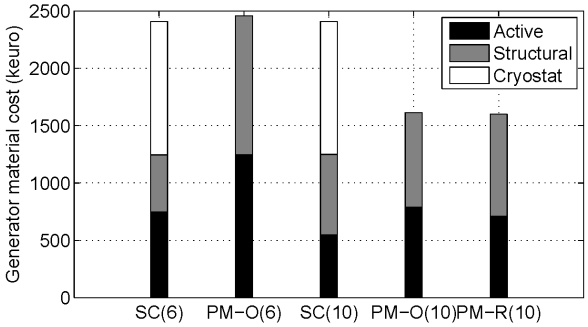

Fig. 9. Generator material costs for SCSGs, PMSG-Os and PMSG-R.

Further cost breakdown for the generator's active material cost is shown in Fig. 10. The SCSGs show their advantage of reducing the active material cost as the required amount of permanent magnets for the PMSGs is rather costly. The total active material of the 10-m SCSG costs the least while the 6-m SCSG is around the same level as the two 10-m PMSGs.

The generator's active material mass, resulting from the optimization merely for the capital CoE, is compared

in Fig. 11. Due to the great amount of iron used to reduce the capital CoE, the SCSGs are rather heavy in this comparison, especially with the air gap diameter of 6 m. The SCSGs do not show effective mass reduction which should have benefited from using superconductors. Using lightweight core materials may help but is beyond the scope of this paper. The PMSGs show light weights with small pole pitches as expected.

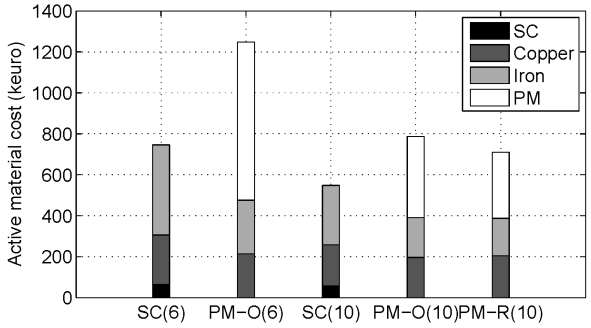

Fig. 10. Active material costs for SCSGs, PMSG-Os and PMSG-R.

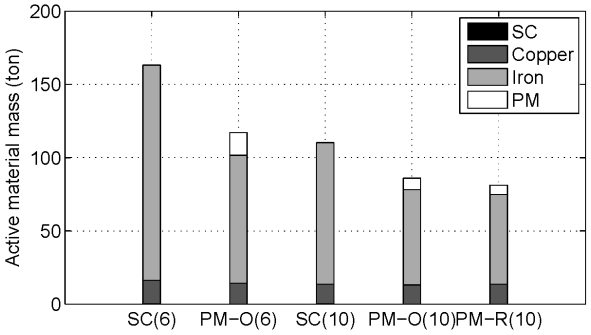

Fig. 11. Active material mass for SCSGs, PMSG-Os and PMSG-R.

For the diameter of 10 m, the PMSG-O is slightly superior to the PMSG-R regarding the CoE and AEP. However, the original 10-m PMSG-R design in [3] will have slightly better performance than the optimized10-m PMSG-O if not adjusted to comply with the conditions and constraints used in this paper, since it was designed for a slightly higher force density and a different turbine.

The SCSGs are not too expensive regarding the capital CoE, compared to their PMSG counterparts. Considering installation, operation and maintenance costs and reliability issues related to realizing super-conduction, however, the SCSGs have not yet shown significant advantages.

V. Conclusions

This paper aims to compare novel SCSGs and conventionally employed PMSGs for 10-MW direct-drive wind turbines. The method of modelling the costs and losses have been presented with certain assumptions and constraints. The comparison results show that the capital CoE of the SCSGs of the air gap diameter of 6 m and 10 m are about 5% higher than that of the PMSG of the air gap diameter of 10 m.

The AEP and CP of the SCSGs are comparable to those of the efficient 10-m PMSGs. All the generators have CPs higher than 0.5 but the 6-m PMSG-O is least efficient. The 10-m PMSGs cost roughly 33% less regarding the total generator material while the 10-m SCSG costs the least regarding the total active material.

In summary, the comparisons show that SCSGs may not be too expensive regarding the capital CoE for 10-MW direct-drive wind turbines. However, the SCSGs may not be competitive yet at the moment if other major costs and reliability factors related to (cooling) superconductors are added to the CoE. Reducing the unit cost of superconducting wires (i.e. MgB_2 in this paper) could be a way to increase the competitiveness but it is beyond the scope of this paper.

References

[1] H. Polinder, J. A. Ferreira, B. B. Jensen, A. B. Abrahamsen, K. Atallah, and R. a. McMahon, "Trends in Wind Turbine Generator Systems," *IEEE J. Emerg. Sel. Top. Power Electron.*, vol. 1, pp. 174–185, 2013.

[2] A. B. Abrahamsen, N. Mijatovic, E. Seiler, T. Zirngibl, C. Træholt, P. B. Nørgård, N. F. Pedersen, N. H. Andersen, and J. Østergård, "Superconducting wind turbine generators," *Supercond. Sci. Technol.*, vol. 23, no. 3, p. 034019, 2010.

[3] H. Polinder, D. Bang, R. P. J. O. M. van Rooij, A. S. McDonald and M. A. Mueller, "10 MW Wind Turbine Direct-Drive Generator Design with Pitch or Active Speed Stall Control," 2007 IEEE International Electric Machines & Drives Conference, Antalya, 2007, pp. 1390-1395.

[4] Innwind.eu [Online]. Available: http://www.innwind.eu/.

[5] H. Li, Z. Chen, and H. Polinder, "Optimization of Multibrid Permanent-Magnet Wind Generator Systems," *IEEE Trans. Energy Convers.*, vol. 24, pp. 82–92, 2009.

[6] C. Stuebig, et al., "Electromagnetic design of a 10 MW permanent magnet synchronous generator for wind turbine application," 2015 IEEE International Electric Machines & Drives Conference (IEMDC), Coeur d'Alene, ID, 2015, pp. 1202-1208.

[7] I. Marino et al., "Lightweight MgB_2 superconducting 10 MW wind generator," *Supercond. Sci. Technol.*, vol. 29, pp. 024005, Feb. 2016.

[8] J. Wang et al., "Comparison study of superconducting wind generators with HTS and LTS field windings," *IEEE Trans. Appl. Supercond.*, vol. 25, no. 3, 2015.

[9] G. Shrestha, "Structural Flexibility of Large Direct Drive Generators for Wind Turbines," Ph. D. dissertation, TU Delft, 2013.

[10] A. Grauers, "Design of direct-driven permanent-magnet generators for wind turbines," Ph.D. dissertation, Chalmers Univ. Technol., Goteborg, Sweden, 1996.

[11] D. Liu, H. Polinder, N. Magnusson, J. Schellevis and A. B. Abrahamsen, "Ripple Field AC Losses in 10-MW Wind Turbine Generators With a MgB_2 Superconducting Field Winding," *IEEE Trans. Appl. Supercond.*, vol. 26, no. 3, pp. 1-5, April 2016.

[12] A. A. Arkadan, R. Vyas, J. G. Vaidya and M. J. Shah, "Effect of toothless stator design and core and stator conductors eddy current losses in permanent magnet generators," *IEEE Trans. Energy Convers.*, vol.7, pp.231-237, Mar 1992.

[13] Fair, R. Superconductivity for Large Scale Wind Turbines, DOE report DE-EE0005143, 2012.

[14] H. Polinder, F. F. Van Der Pijl, G. J. De Vilder, and P. J. Tavner, "Comparison of direct-drive and geared generator concepts for wind turbines," *IEEE Trans. Energy Convers.*, vol. 21, pp. 725–733, 2006.